First Bistatic Spaceborne SAR Experiments With TanDEM-X

Marc Rodriguez-Cassola, Pau Prats, *Member, IEEE*, Daniel Schulze, Nuria Tous-Ramon, Ulrich Steinbrecher, Luca Marotti, Matteo Nannini, Marwan Younis, Paco López-Dekker, *Member, IEEE*, Manfred Zink, Andreas Reigber, *Senior Member, IEEE*, Gerhard Krieger, *Senior Member, IEEE*, and Alberto Moreira, *Fellow, IEEE*

***Abstract*—TanDEM-X (TerraSAR-X Add-on for Digital Elevation Measurements) is a high-resolution interferometric mission with the main goal of providing a global and unprecedentedly accurate digital elevation model of the Earth surface by means of single-pass X-band synthetic aperture radar (SAR) interferometry. Despite its usual quasi-monostatic configuration, TanDEM-X is the first genuinely bistatic SAR system in space. During its monostatic commissioning phase, the system has been mainly operated in pursuit monostatic mode. However, some pioneering bistatic SAR experiments with both satellites commanded in nonnominal modes have been conducted with the main purpose of validating the performance of both space and ground segments in very demanding scenarios. In particular, this letter reports about the first bistatic acquisition and the first single-pass interferometric (mono-/bistatic) acquisition with TanDEM-X, addressing their innovative aspects and focusing on the analysis of the experimental results. Even in the absence of essential synchronization and calibration information, bistatic images and interferograms with similar quality to pursuit monostatic have been obtained.**

***Index Terms*—Bistatic radar, bistatic SAR processing, spaceborne SAR missions, synthetic aperture radar (SAR), time and phase synchronization.**

I. Introduction

THE FIRST bistatic synthetic aperture radar (SAR) system in space is TanDEM-X,[1] whose main goal is the generation of a global digital elevation model (DEM) following the High-Resolution Terrain Information-3 (HRTI-3) standard [1]. TanDEM-X extends the TerraSAR-X mission by adding a second fully active satellite with cooperative operation capabilities, forming a single-pass interferometric system, and is therefore capable of providing very accurate 3-D information. During the first years of the TerraSAR-X mission, the German Aerospace Center (DLR) has benefitted from the flexibility of the system to perform some innovative SAR experiments in nonnominal configurations, i.e., spaceborne–airborne bistatic imaging [2] or the demonstration of new imaging modes [3]. The uniqueness and the increased operational possibilities of the new mission allow one to envisage a large amount of challenging and creative experiments to take advantage of the potential of the payloads. Aside from the obvious goal of testing the performance of the system in nonnominal bistatic configurations, a further objective should be outlined: develop and test new techniques, modes, or algorithms which might become relevant in future SAR missions.

This letter addresses the first bistatic experiments performed with TanDEM-X during its monostatic commissioning phase: 1) the first bistatic acquisition, complemented with a repeat-pass interferometric processing of consecutive bistatic surveys and 2) the first single-pass bistatic interferometric acquisition.

II. TanDEM-X in the Pursuit Monostatic Commissioning Phase

For approximately one month, TDX followed a specific test schedule while approaching TSX from the original 16 000 km to the final flight formation with 20-km separation planned for the monostatic commissioning phase. Both satellites operated independently in pursuit monostatic mode for the following months, TDX completing a monostatic test program to validate its expected performance. The monostatic commissioning phase ended in early October 2010, after which TDX approached TSX to a distance of some hundred meters to achieve the so-called close flight formation. In this configuration, and from a purely geometrical point of view, TanDEM-X can be well considered as monostatic.

Despite the tight operational schedule, some room was reserved for innovative experiments during the first months of the mission. As an example, the first interferometric experiment was carried out on July 16, while TDX and TSX were still separated by 370 km [4]. Some two weeks later, the first bistatic acquisition of TDX was conducted. The monostatic commissioning phase was very appealing to perform nonnominal bistatic SAR experiments because of the longer along-track baselines. It has been under these circumstances that the first bistatic experiments with TanDEM-X have been conducted. Fig. 1 shows the reference configuration formed by the TSX and TDX satellites at the period.

III. Experimental Results

As previously stated, two sets of innovative bistatic experiments have been carried out during the monostatic

Manuscript received April 6, 2011; accepted May 12, 2011. Date of publication August 1, 2011; date of current version December 23, 2011.

The authors are with the Microwaves and Radar Institute, German Aerospace Center (DLR), 82234 Oberpfaffenhofen, Germany (e-mail: Marc.Rodriguez@dlr.de; pau.prats@dlr.de; Daniel.Schulze@dlr.de; ulrich.steinbrecher@dlr.de; marwan.younis@dlr.de; Francisco.dekker@dlr.de; manfred.zink@dlr.de; andreas.reigber@dlr.de; gerhard.krieger@dlr.de; alberto.moreira@dlr.de).

Color versions of one or more of the figures in this paper are available online at http://ieeexplore.ieee.org.

Digital Object Identifier 10.1109/LGRS.2011.2158984

[1]TanDEM-X, acronym for **T**erraSAR-X **A**dd-o**n** for **D**igital **E**levation **M**easurements, is the name of the mission; in addition, it is also the name with which the second satellite is commonly referred to at DLR. To avoid ambiguities, we will refer to this second satellite as TDX; analogously, the TerraSAR-X satellite is referred to as TSX.

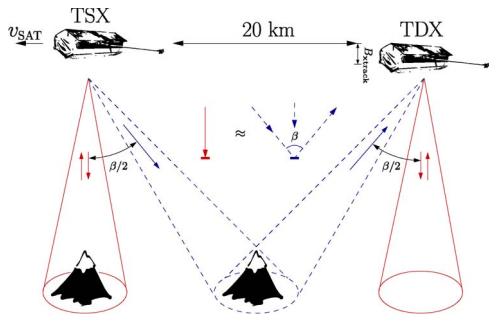

Fig. 1. Formation of the TSX and TDX satellites during the TanDEM-X monostatic commissioning phase.

TABLE I
ACQUISITION PARAMETERS

	Experiment 1	Experiment 2
PRF [Hz]	3182.52	2991.24 × 2
Tx bandwidth [MHz]	100	150
Incident angle [deg]	36.6	35.8
Squint angle TSX/TDX [deg]	±0.8	±0.9
Bistatic swath [km]	68.44	14.58
Cross-track baseline [m] (B_{xtrack})	253	43
Polarisation	VV	HH

commissioning phase. In both cases, the geometrical configuration coincided with the one shown in Fig. 1: The beams used in pursuit monostatic operation are represented by solid lines; the dashed ones correspond to a bistatic operation with symmetric azimuth steering. Table I lists the main parameters of the acquisitions. The column "Experiment 1" refers to the first bistatic imaging acquisition, with which the repeat-pass bistatic interferometric results were produced; the column "Experiment 2" refers to the first single-pass bistatic interferometric acquisition. All data takes were acquired using the regular strip-map modes of the satellites. The data have been processed using the experimental **Ta**nDEM-**X i**nterferometric processor (TAXI), which is a flexible and versatile processing suite particularly developed for the evaluation of TanDEM-X experimental data products [5], [6].

A. Experiment 1: Bistatic Imaging and Repeat-Pass Interferometry

The acquisition, carried out for the first time on August 8, 2010, was planned over Brasilia city, Brazil [7]. For this first bistatic experiment, TSX operated monostatically with a squint of -0.8°, whereas TDX was set in receive-only mode with a squint of 0.8°. Due to the small bistatic angle, no relevant modifications of the timing schemes were required. Synchronization pulses were exchanged during the data take using the TanDEM-X direct link (SyncLink), from which the differential clock error could be measured [1]. A squinted monostatic image and a nonsquinted bistatic one were obtained, but with no spectral overlap between them. The same acquisitions were conducted in consecutive passes of the system over the same area to produce bistatic repeat-pass interferograms, i.e., after 11 days.

The first bistatic image acquired by TanDEM-X is shown in Fig. 2, where the famous airplane-like shape of the Brazilian capital appears in the center of the image. The color coding is used to discriminate homogeneous areas (bluish color in the image) from structured areas (yellowish color in the image). For better comparison with the monostatic image, Fig. 3 shows a zoom over the city with the monostatic and the bistatic images overlaid and appearing in magenta and green, respectively. Two different aspects of the previous images can be outlined. In the city center, the dominant scattering mechanism seems to be monostatic, but there exist distinct building areas near the lake, where the bistatic scattering dominates. The conclusion is that, even for the small bistatic angle of the experiment, which is about 1.6°, significant changes in target reflectivity, particularly in man-made structures, can be expected between monostatic and bistatic observations. This feature might be very helpful to enhance the performance of existing identification or classification algorithms. The second one is the distribution of the azimuth ambiguities. Considering the azimuth ambiguities of the point target of opportunity in the center of Fig. 3, which are mapped on the lake and zoomed within the ochre rectangle at the bottom right corner of the figure, a range difference in the positions of the monostatic and bistatic ambiguities appears.

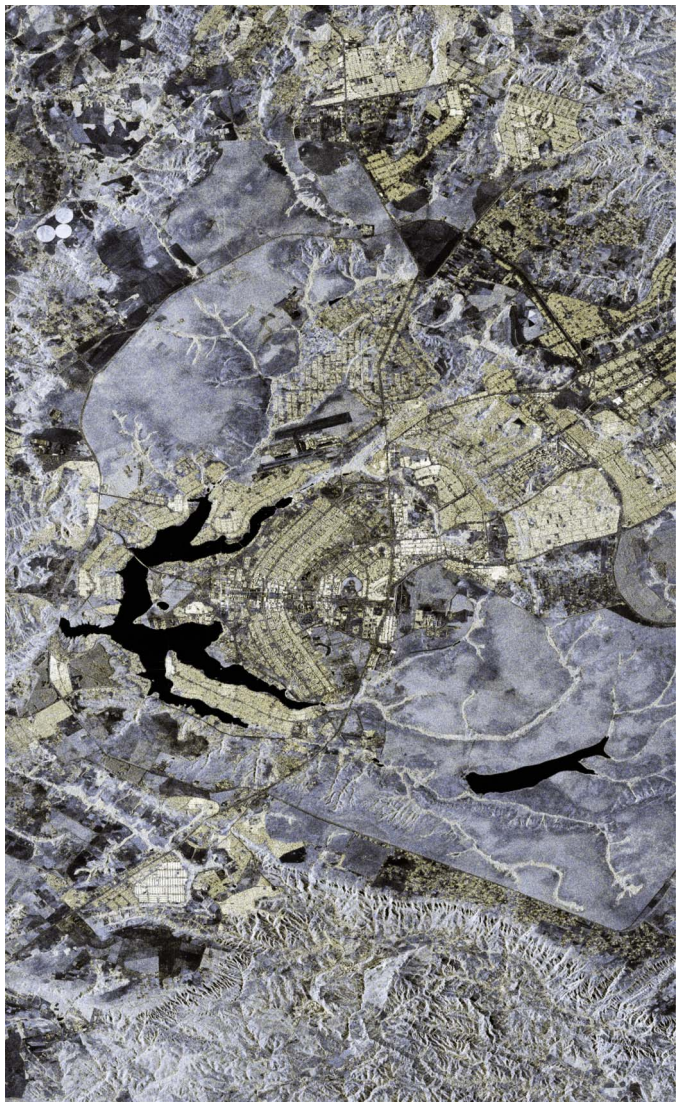

Fig. 2. First TanDEM-X bistatic image, showing the Brasilia city area in radar coordinates (horizontal bistatic range; vertical azimuth time). Bistatic range increases from left to right. Color coding is used to distinguish (bluish color) homogeneous areas from (yellowish color) structured areas.

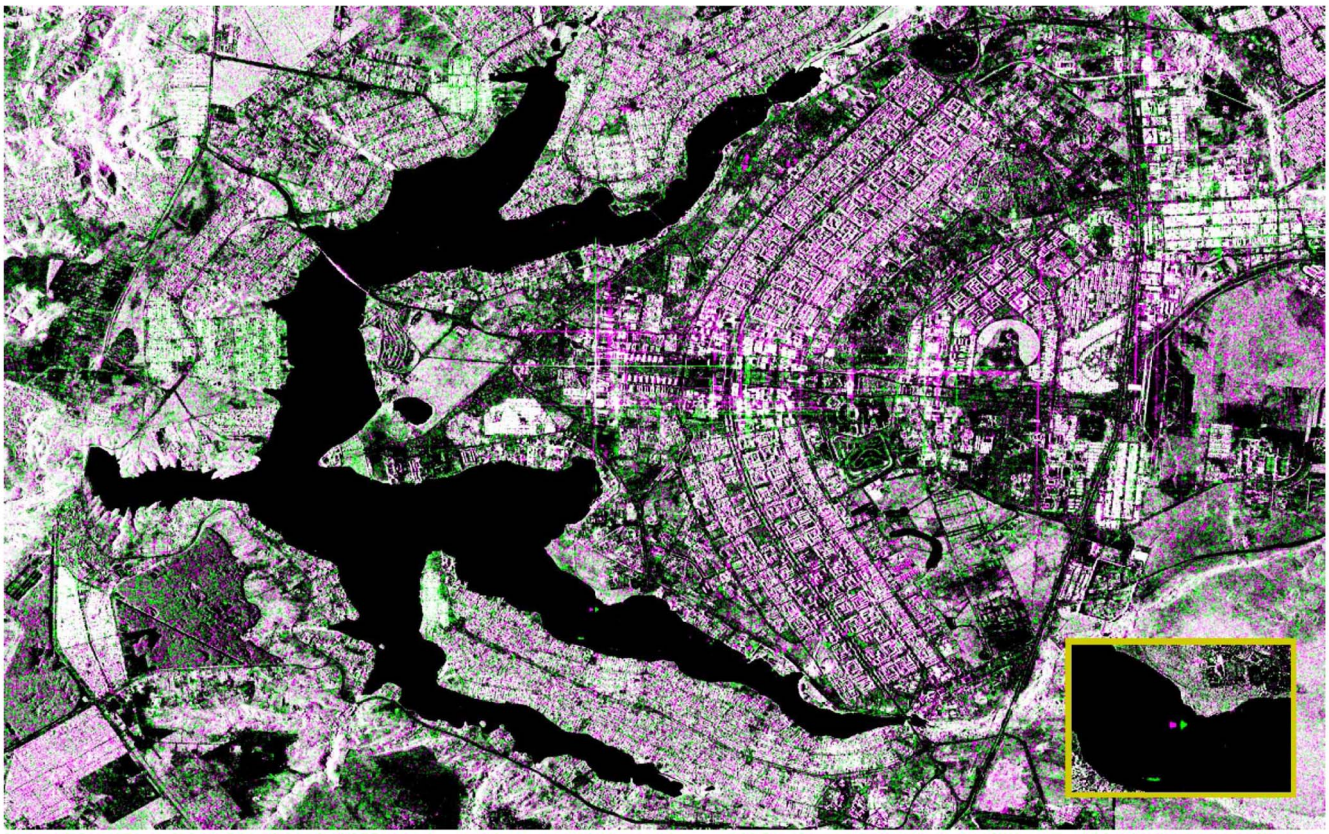

Fig. 3. Zoom over Brasilia. (Green) TanDEM-X bistatic over (magenta) TerraSAR-X monostatic. Radar coordinates (horizontal range; vertical azimuth time). Radar illumination from the left. Note the significant differences in the scattering of some buildings between the monostatic and bistatic images. Note also the different range positions of the ambiguities of the images as a consequence of the different squint angles (see rectangle at the bottom right).

This happens because the monostatic image is squinted whereas the bistatic is not, and therefore, the 2-D monostatic impulse response, unlike the monostatic, is skewed. This feature might be exploited to develop ambiguity identification/suppression strategies.

Fig. 4 shows the repeat-pass interferogram generated with two bistatic images acquired with a time lag of 11 days. Note that the images are rotated 90° with respect to Figs. 2 and 3. Before interferometric combination, the bistatic data have been calibrated in phase and time with the use of the SyncLink (cf. Section III-B) information [1]. The SRTM (Shuttle Radar Topography Mission) DEM has been used to remove topography [8]. The residual fringes correspond mainly to *a priori* DEM errors and (possibly) marginally to unaccounted atmospheric effects. The mean value of the coherence is 0.35; in urban areas, this value increases to about 0.5. There are no significant differences between the values obtained from the monostatic repeat-pass and the bistatic interferograms. Concerning the interferometric performance, the baselines are practically the same, as is the SNR of both acquisitions. Note that the monostatic image has a squint, but since no significant changes in target reflectivity other than those for certain man-made structures have been observed, the results are definitely consistent. Aside from its novelty, the relevant conclusion of this experiment was that we could obtain with the new system bistatic images and interferograms of similar quality to the monostatic (more mature) TerraSAR-X counterparts, a quite relevant information at the time.

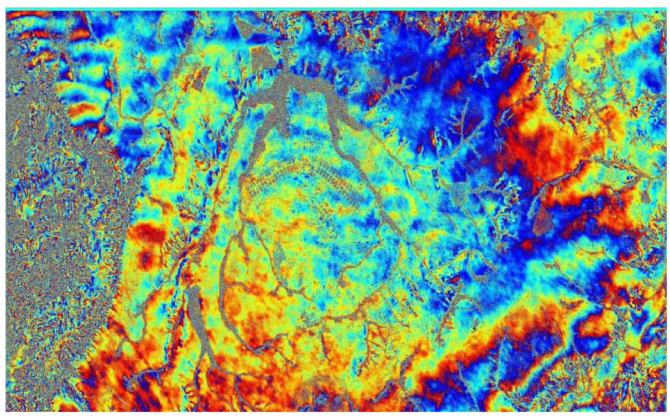

Fig. 4. Bistatic repeat-pass interferogram generated with two bistatic images over Brasilia with a time lag of 11 days. Radar coordinates (vertical range; horizontal azimuth time). Radar illumination from the top.

B. Experiment 2: Bistatic Single-Pass Interferometry

Following the success of the bistatic imaging acquisitions (cf. Section III-A), a natural step was to perform a single-pass bistatic interferometric experiment before the end of the pursuit monostatic commissioning phase, i.e., profiting of the 20-km along-track baseline. However, a way to overcome the spectral decorrelation of the previous bistatic configuration was needed. Because of the small bistatic angle, simultaneous monostatic and bistatic images with similar equivalent squint angles have Doppler spectral overlap, which further suggests coherence

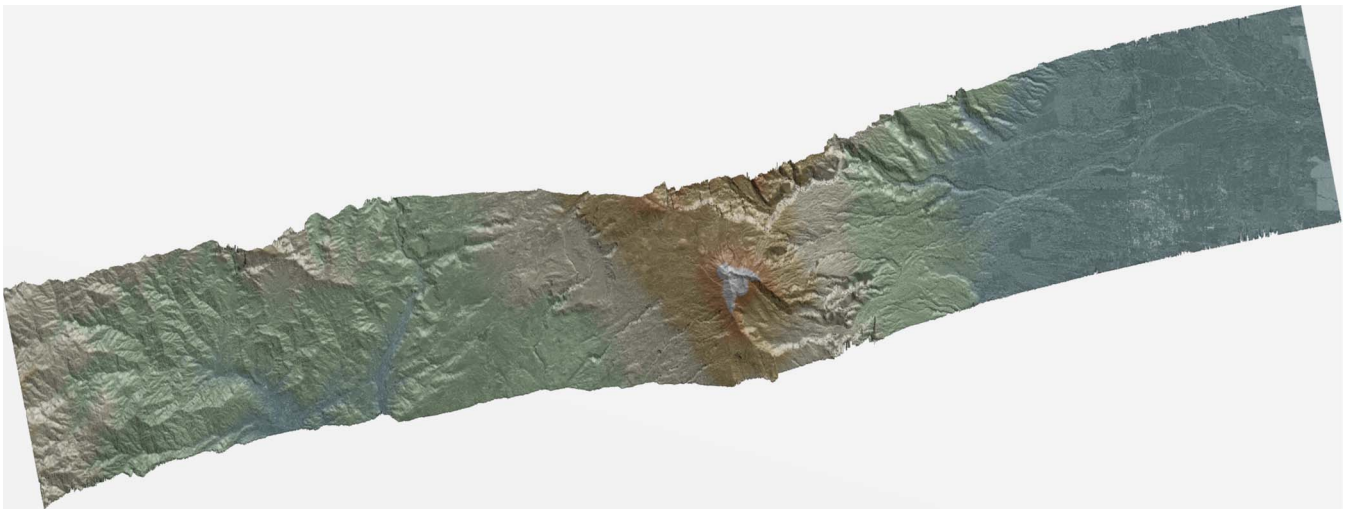

Fig. 5. Geocoded (north points rightward) DEM of the area surrounding the Turrialba volcano, the first single-pass bistatic interferometric TanDEM-X acquisition. The figure shows the color-coded height with the bistatic reflectivity overlaid.

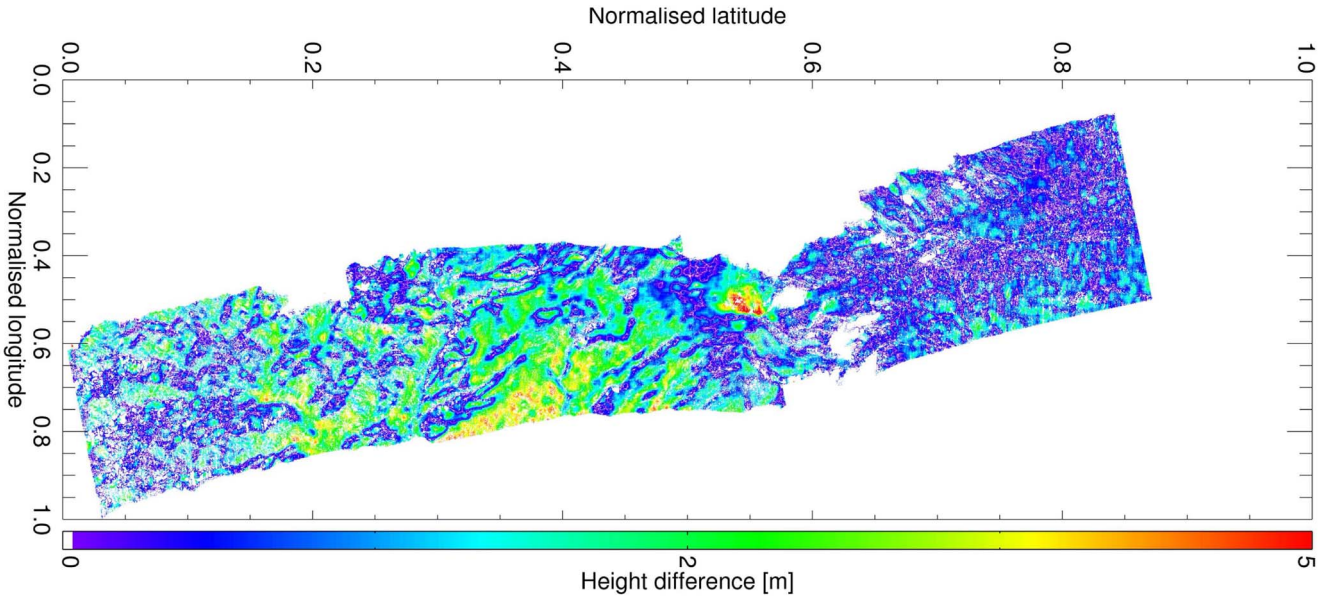

Fig. 6. Difference between pursuit monostatic and single-pass bistatic DEMs. A multilook with an effective factor of 20 has been applied to the data.

between the two images. This equivalence is shown in Fig. 1. To achieve this, an imaginative command of the satellites was designed, with a switch of the azimuth antenna patterns of TSX and TDX on a pulse-to-pulse basis. Both satellites transmitted one pulse using the nonsquinted beams (solid lines) in Fig. 1 (any undesired energy from the other satellite was highly attenuated due to the lack of overlap of the nonsquinted footprints, separated by about 17 km); in the next pulse, TSX transmitted with a squint of -0.9°, and TDX only received with a squint of $+0.9^\circ$ (depicted with the dashed lines in Fig. 1). All things considered, one pursuit monostatic interferogram with full baseline, plus two symmetric bistatic interferograms with half baseline, could be computed.[2] However, the acquisition had a couple of drawbacks: First, the PRF needed to be doubled, i.e., the swath was halved, and second, due to the specifics of the command, no calibration nor synchronization pulses were available. The acquisition was carried out over the *Parque Nacional del Volcán Turrialba* in Costa Rica, which is a gracefully mountainous area. Note that this experiment was conducted in early October 2010, which is about a week before the first official bistatic TanDEM-X interferograms in close formation were obtained, and is therefore the first bistatic single-pass spaceborne SAR interferometric acquisitions.

TanDEM-X incorporates a direct X-band link (SyncLink) to calibrate the time and phase references of the bistatic data, so that no residual synchronization errors propagate in the final DEM product [9]. As a matter of fact, without proper clock synchronization, no bistatic SAR interferometry is possible [10]. In the absence of SyncLink information, TAXI has an automatic synchronization module which is capable of recovering the synchronization error using the bistatic data [11], [12], which definitely substantiates the scientific character of the experiment. The estimated clock carrier frequency difference of about 124 Hz is also consistent with the available contemporary SyncLink samples.

[2]Note that the acquisition differed from a ping-pong one in which the two monostatic images were not consecutive (one pulse delay) but simultaneous; moreover, only a single bistatic image (instead of two) was acquired.

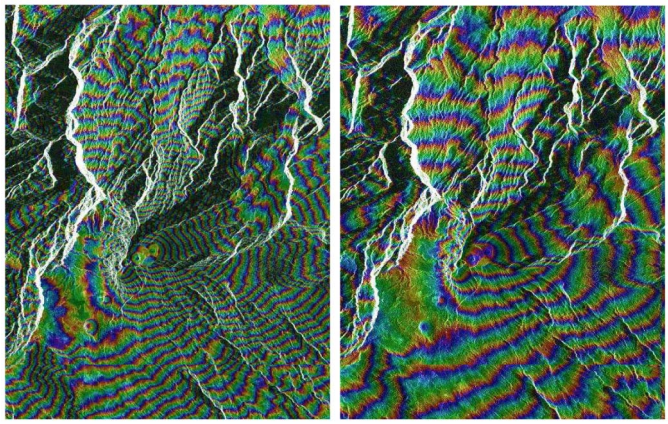

Fig. 7. Crop of the interferograms in the areas surrounding the volcano. (Left) Pursuit monostatic and (right) single-pass bistatic interferograms. Note the higher sensitivity to topography of the pursuit monostatic interferogram due to the higher baseline.

Fig. 5 shows the DEM generated using one of the bistatic interferograms (with bistatic reflectivity overlaid). Although the test of the performance of this automatic synchronization procedure is out of the scope of this letter, we can show the validity of the approach by cross-checking the results obtained using the single-pass bistatic interferogram of Fig. 5 and the one resulting from the conventional pursuit monostatic one. Fig. 6 shows the height difference between the two DEMs. A mask has been used to avoid including values with low coherence. No trends in range or azimuth can be identified, which qualitatively validates the automatic synchronization approach. The standard deviation of the height error of the DEMs computed using single-look interferograms is 23.3 m, which results in an effective averaging factor of about 20 for the DEM error of the figure.

Fig. 7 shows a crop of the (left) pursuit monostatic interferogram and (right) one bistatic flattened interferogram showing an area near the volcano. As expected, the pursuit monostatic interferogram has twice as much height sensitivity as the bistatic. The height of ambiguity of the pursuit monostatic acquisition is about 85 m. In terms of coherence, we expect the mono-/bistatic pairs to be less sensitive to volume decorrelation because of the halved baseline. Nevertheless, the bistatic image is also expected to have an SNR 1.2 dB worse for equivalent reflectivity. This loss in SNR is attributed mainly to the electronic antenna steering and consequently causes a proportional loss of the overall coherence in the mono-/bistatic pairs. The mean value of the coherence of the pursuit monostatic pair is 0.65; for the single-pass bistatic pairs, this value drops to about 0.63. To illustrate the impact of volume decorrelation in the pursuit monostatic and one single-pass bistatic acquisitions, Fig. 8 shows the interferometric coherences (middle—pursuit monostatic; right—single-pass bistatic) in a forest area north from the volcano; the left crop corresponds to the bistatic intensity image. Although not blatantly evident, the forest area has a lower coherence in the pursuit monostatic pair due to volumetric decorrelation.

IV. Summary

This letter has presented two innovative spaceborne SAR experiments performed with TanDEM-X in the monostatic commissioning phase of the mission (in particular, the first bistatic imaging acquisitions and the first single-pass bistatic interferometric acquisition). Moreover, repeat-pass bistatic interferometry with TanDEM-X has also been demonstrated. Even in these experimental configurations, with partial lack of synchronization and calibration information, bistatic interferograms of similar quality to the monostatic ones have been produced.

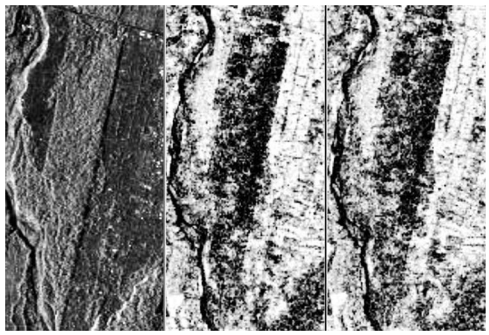

Fig. 8. Forest area north from the volcano. The left plot shows the bistatic intensity image of the area. The middle and right plots show the pursuit monostatic and single-pass bistatic coherences, respectively. Note the decrease in the coherence of the middle crop w.r.t. the right crop, caused by volumetric decorrelation.

References

[1] G. Krieger, A. Moreira, H. Fiedler, I. Hajnsek, M. Werner, M. Younis, and M. Zink, "TanDEM-X: A satellite formation for high-resolution SAR interferometry," *IEEE Trans. Geosci. Remote Sens.*, vol. 45, no. 11, pp. 3317–3341, Nov. 2007.

[2] M. Rodriguez-Cassola, S. V. Baumgartner, G. Krieger, and A. Moreira, "Bistatic TerraSAR-X/F-SAR spaceborne–airborne experiment: Description, data processing and results," *IEEE Trans. Geosci. Remote Sens.*, vol. 48, no. 2, pp. 781–794, Feb. 2010.

[3] P. Prats, R. Scheiber, J. Mittermayer, A. Meta, and A. Moreira, "Processing of sliding spotlight and TOPS SAR data using baseband azimuth scaling," *IEEE Trans. Geosci. Remote Sens.*, vol. 48, no. 2, pp. 770–780, Feb. 2010.

[4] P. López-Dekker, P. Prats, F. De Zan, D. Schulze, G. Krieger, and A. Moreira, "TanDEM-X first DEM acquisition: A crossing orbit experiment," *IEEE Geosci. Remote Sens. Lett.*, vol. 8, no. 5, pp. 943–947, Sep. 2011.

[5] P. Prats, M. Rodriguez-Cassola, L. Marotti, M. Naninni, S. Wollstadt, D. Schulze, N. Tous-Ramon, M. Younis, G. Krieger, and A. Reigber, "TAXI: A Versatile Processing Chain for Experimental TanDEM-X Product Evaluation," in *Proc. IGARSS*, Honolulu, HI, 2010, pp. 4059–4062.

[6] *TanDEM-X Science Web Site*. [Online]. Available: www.dlr.de/hr/tdmx/

[7] *TanDEM-X Mission Blog*. [Online]. Available: www.dlr.de/blogs/desktopdefault.aspx/tabid-5919/9754_read-245/

[8] T. G. Farr, P. A. Rosen, E. Caro, R. Crippen, R. Duren, S. Hensley, M. Kobrick, M. Paller, E. Rodriguez, L. Roth, D. Seal, S. Shaffer, J. Shimada, J. Umland, M. Werner, M. Oskin, D. Burbank, and D. Alsdorf, "The Shuttle Radar Topography Mission," *Rev. Geophys.*, vol. 45, p. RG2004, May 2007.

[9] M. Younis, R. Metzig, and G. Krieger, "Performance prediction of a phase synchronization link for bistatic SAR," *IEEE Geosci. Remote Sens. Lett.*, vol. 3, no. 3, pp. 429–433, Jul. 2006.

[10] H. Cantalloube, M. Wendler, V. Giroux, P. Dubois-Fernandez, and G. Krieger, "Challenges in SAR processing for airborne bistatic acquisitions," in *Proc. EUSAR*, Ulm, Germany, 2004, pp. 1–4.

[11] M. Rodriguez-Cassola, P. Prats, L. Marotti, M. Naninni, M. Younis, G. Krieger, and A. Reigber, "A versatile processing chain for experimental TanDEM-X product evaluation," in *Proc. EUSAR*, Aachen, Germany, 2010, pp. 1–4.

[12] M. Rodriguez-Cassola, P. Prats, P. Lopez-Dekker, G. Krieger, and A. Moreira, "General processing approach for bistatic SAR systems: Description and performance analysis," in *Proc. EUSAR*, Aachen, Germany, 2010, pp. 1–4.